

ELASTIC PLASTIC ANALYSIS OF GROWING CRACKS

by J.R. Rice, W.J. Drugan and T.L. Sham

Division of Engineering, Brown University, Providence, R.I. 02912

May 1979

NOTICE  
This report was prepared as an account of work sponsored by the United States Government. Neither the United States nor the United States Department of Energy, nor any of their employees, nor any of their contractors, subcontractors, or their employees, makes any warranty, express or implied, or assumes any legal liability or responsibility for the accuracy, completeness or usefulness of any information, apparatus, product or process disclosed, or represents that its use would not infringe privately owned rights.

This paper was presented at the ASTM 12th Annual Symposium on Fracture Mechanics, Washington University, St. Louis, 21-23 May 1979; submitted to ASTM for publication.

## **DISCLAIMER**

**This report was prepared as an account of work sponsored by an agency of the United States Government. Neither the United States Government nor any agency Thereof, nor any of their employees, makes any warranty, express or implied, or assumes any legal liability or responsibility for the accuracy, completeness, or usefulness of any information, apparatus, product, or process disclosed, or represents that its use would not infringe privately owned rights. Reference herein to any specific commercial product, process, or service by trade name, trademark, manufacturer, or otherwise does not necessarily constitute or imply its endorsement, recommendation, or favoring by the United States Government or any agency thereof. The views and opinions of authors expressed herein do not necessarily state or reflect those of the United States Government or any agency thereof.**

## **DISCLAIMER**

**Portions of this document may be illegible in electronic image products. Images are produced from the best available original document.**

ELASTIC PLASTIC ANALYSIS OF GROWING CRACKS\*

by J. R. Rice, W. J. Drugan and T. L. Sham

Division of Engineering, Brown University, Providence, RI 02912

May 1979

Abstract

In an extension of earlier studies by Rice and Sorensen, we discuss the elastic-plastic stress and deformation fields at the tip of a crack which grows in an ideally plastic solid under plane strain, small scale yielding conditions. The results of an asymptotic analysis suggest the existence of a crack tip stress state similar to that of the classical Prandtl field, but containing a zone of elastic unloading between the centered fan region and the trailing constant stress plastic region. The near tip expression for the rate of opening displacement  $\dot{\delta}$  at distance  $r$  from the growing tip is found to have the same form suggested by Rice and Sorensen,

$$\dot{\delta} = \alpha \dot{J}/\sigma_0 + \beta(\sigma_0/E) \dot{a} \ln(R/r)$$

but now the presence of the elastic wedge causes  $\beta$  to have the revised value of 5.08 (for Poisson ratio  $\nu = 0.3$ ). Here,  $a$  = crack length,  $\sigma_0$  = yield strength,  $E$  = elastic modulus, and  $J$  denotes the far-field value, namely  $(1-\nu^2)K^2/E$  for the small scale yielding conditions considered. The parameters  $\alpha$  and  $R$  cannot be determined from the asymptotic analysis, but comparisons with finite element solutions suggest that, at least for small amounts of growth,

---

\*Presented at ASTM 12th Annual Symposium on Fracture Mechanics, Washington University, St. Louis, 21-23 May 1979; submitted to ASTM for publication.

$\alpha$  is approximately the same for stationary and growing cracks, and  $R$  scales approximately with the size of the plastic zone, being about 15% to 30% larger. For large scale yielding it is argued that a similar form applies with possible variations in  $\alpha$  and  $\beta$ , at least in cases which maintain triaxial constraint at the crack tip, but in the fully yielded case  $R$  is expected to be proportional to the dimension of the uncracked ligament. The model crack growth criterion of Rice and Sorensen, requiring a critical  $\delta$  at some fixed  $r$  from the tip, is re-examined in light of the more accurate solution. The results suggest that the  $J$  versus  $\Delta a$  relation describing growth will be dependent on the extent of yielding, although it is suggested that this dependency might be small for highly ductile materials, provided that a similar triaxial constraint is maintained in all cases.

## Introduction

The aim of the paper is to describe recent studies on the stress and deformation fields at growing plane strain crack tips in elastic-ideally plastic solids, and to interpret the results in terms of criteria for stable crack growth. In both respects the work is an extension of a recently published study by Rice and Sorensen [1] (henceforth denoted RS for brevity).

In the next section we present the principal results of a recent analysis [2] of the asymptotic stress field at a growing crack tip where we find, contrary to the assumption of RS, that a full Prandtl field cannot exist at the tip but, rather, its "centered fan" and trailing "constant stress" sectors are divided by an elastic unloading zone. The net stress triaxiality in front of the crack and, indeed, the entire near tip stress distribution differs little from that of the Prandtl field, which may explain why the effect was not revealed in previous finite element simulations of crack growth [3,1]. We find the same expression as RS did for the asymptotic form of the near tip openings, but with a revised value of their parameter  $\beta$  (see eqs. 19,21).

The following section analyzes recent finite element studies [4] of (limited amounts of) stable crack growth under small scale yielding conditions, based on a refinement of mesh size as suggested in RS to more accurately determine parameters such as  $R$  and  $\alpha$  (again, see eqs. 19,21) in their expression for the near-tip crack openings. The asymptotic and finite element results seem to be consistent with one another, and together they provide a reasonably complete understanding of the near tip field, at least for limited amounts of stable growth, although numerical results still leave some uncertainties in the determination of  $\alpha$  and  $R$ .

Subsequent portions of the paper examine a criterion for crack growth, in the form suggested in RS, requiring that a fixed crack surface

opening  $\delta_c$  be maintained at a small characteristic distance  $r_m$  (intended to coincide approximately with a "fracture process zone" size) from the tip for continuing growth. Crack growth, under small scale yielding, is discussed based on the criterion and, in addition, we discuss some possible implications of the criterion for large scale yielding (but in geometries like deeply-cracked bend specimens, maintaining a crack tip triaxial constraint similar to that of the Prandtl field even under fully yielded conditions).

Our considerations suggest a dependence of the  $J$  versus crack growth ( $\Delta a$ ) relation on the extent of yielding, although for highly ductile materials (large values of the Paris tearing modulus  $T$  [5,6]) these dependencies might sometimes be relatively small. An Appendix to the paper compares some possible definitions of  $J$  for fully plastic specimens.

Asymptotic Near-Tip Fields for Stationary and Growing Cracks

Rice [7,8] and Hutchinson [9] have constructed asymptotic plane strain crack tip stress states for ideally plastic solids by slip line methods, and have analyzed the nature of the strain singularities within "centered fan" sectors for loading of a stationary crack. Similar methods have been adopted for growing cracks, where the nature of the elastic-plastic strain singularity in centered fan sectors moving with the tip has been discussed by Rice [8,10], Cherepanov [11], and by RS.

For our present discussion it is convenient to follow a development of Rice and Tracey [12] which analyzed directly, within conventional "small strain" assumptions, the stress state  $\sigma_{ij} = \sigma_{ij}(\theta)$  resulting as  $r \rightarrow 0$  at the tip of a crack in an ideally plastic solid under plane strain conditions ( $r, \theta$  are polar coordinates centered on the tip as in fig. 1a). They observe first that since the stress at the tip must be bounded, terms of the form  $r \partial \sigma_{ij} / \partial r$  in the stress equilibrium equations must vanish as  $r \rightarrow 0$ , and hence the equilibrium equations reduce to the two ordinary differential equations

$$\sigma_{rr} - \sigma_{\theta\theta} + d\sigma_{r\theta}/d\theta = 0, \quad (1)$$

$$2\sigma_{r\theta} + d\sigma_{\theta\theta}/d\theta = 0. \quad (2)$$

Also, they assume that the plastic yield condition in highly strained material at the tip reduces to the form

$$(\sigma_{\theta\theta} - \sigma_{rr})^2/4 + \sigma_{r\theta}^2 = \sigma_0^2/3; \quad (3)$$

that is, that the maximum shear stress in the plane of straining is limited to



the yield in shear,  $\sigma_0/\sqrt{3}$  (where, using the Mises shear to tension conversion,  $\sigma_0$  is the tensile yield strength).

Equation (3) can either be accepted as an approximate criterion of plane strain yielding or can be motivated in the following way. The three-dimensional Prandtl-Reuss-Mises theory is based on the plastic flow rule

$$D_{ij}^p = \Lambda s_{ij} \quad \text{where} \quad \Lambda = \sqrt{D_{ij}^p D_{ij}^p / s_{mn} s_{mn}} \geq 0, \quad (4)$$

$s_{ij}$  is the deviatoric part of  $\sigma_{ij}$ , and  $D_{ij}^p$  is the plastic part of the strain rate tensor  $D_{ij}$ . The latter is defined (relative to Cartesian coordinates  $x_1, x_2, x_3$ ) by

$$2D_{ij} = \partial v_i / \partial x_j + \partial v_j / \partial x_i, \quad (5)$$

where  $v_i$  is the velocity  $\dot{u}_i$  ( $u_i$  is the displacement and the superposed dot means time derivative), and consists of elastic and plastic parts such that

$$D_{ij} = D_{ij}^e + D_{ij}^p = \frac{1+\nu}{E} \dot{\sigma}_{ij} - \frac{\nu}{E} \delta_{ij} \dot{\sigma}_{kk} + \Lambda s_{ij} \quad (6)$$

for isotropic elastic response. For elastic loading or unloading the term with  $\Lambda$  is deleted. In the ideally plastic case  $\Lambda$  is not determined directly by the stress rates, but variations in stress during plastic response must satisfy the yield condition

$$s_{ij} s_{ij} / 2 = \sigma_0^2 / 3. \quad (7)$$

In plane strain, if  $s_{zz} = 0$  (where the  $z$  axis is perpendicular to the  $x,y$  plane of deformation), eq. (7) reduces to eq. (3). Now, by eq. (4) it is clear that whenever

$$D_{zz}^P / \sqrt{D_{ij}^P D_{ij}^P} = 0, \quad (8)$$

$s_{zz} = 0$ , so that eq. (3) results. But since the plane strain crack tip is expected to be the site of a plastic strain singularity, while the plastic strain in the  $z$ -direction is bounded (since total  $z$  strain and its elastic portions are bounded), we expect eq. (8) to be asymptotically valid as  $r \rightarrow 0$ , so that eq. (3) becomes the appropriate form of the yield condition at the tip. This argument is suggestive but not fully satisfactory because, as will be seen, the assumption of eq. (3) leads to the possibility of "constant stress" angular sectors at the tip, which do not produce unbounded plastic strain. Nevertheless, we continue by assuming that eq. (3) is valid within plastically deforming zones at the tip, noting that it must be valid within singular sectors and that the arguments based on it lead to fields in agreement with numerical finite element solutions [12] for the now well-documented case of loading of a stationary crack.

Rice and Tracey [12] showed that the only solutions of the equilibrium equations (1,2), valid within plastic regions at the tip for which eq. (3) is met are of the following types:

(a) Centered fan sectors, in which

$$\sigma_{r\theta} = \pm \sigma_0 / \sqrt{3}, \quad \sigma_{rr} = \sigma_{\theta\theta} = \text{constant} + (2\sigma_0 / \sqrt{3}) \theta, \quad (9)$$

and which have the interpretation in terms of slip lines shown in fig. 1a;

or

(b) Constant stress sectors, in which stresses  $\sigma_{xx}$ ,  $\sigma_{xy}$ ,  $\sigma_{yy}$  (i.e., referred to Cartesian coordinates) are independent of  $\theta$  and meet eq. (3); these have the interpretation in terms of slip lines shown in fig. 1b.

Hence the crack tip stress state consists of an array of plastic angular sectors of type (a) and/or (b), among or between which there may be sectors that respond elastically (or currently respond elastically, but may previously have been yielded).

If we seek a solution of the equilibrium equations (1,2) corresponding to plastic response at all angles  $\theta$  about the tip, then the only solution corresponding to Mode I loading for which all stresses are continuous (note: equilibrium considerations alone require continuity of  $\sigma_{\theta\theta}$  and  $\sigma_{r\theta}$ , but not  $\sigma_{rr}$ ) is that of the Prandtl field shown in fig. 1c. This field was hypothesized by Rice [7,8] as the near tip solution for well-contained yielding; it is known to result as the non-hardening limit of the Hutchinson-Rice-Rosengren [13,14] singularities and seems to be well substantiated by numerical solutions for small scale yielding at a stationary crack tip [12]. (On the other hand, it is known that fully plastic solutions for non-hardening materials show a wide variety of crack tip stress fields, some of which involve discontinuities in  $\sigma_{rr}$  and angular sectors that are stressed below yield).

It was assumed in RS and previous studies of growth [8,10,11] that the same Prandtl field of fig. 1c provides the stress state at a growing crack tip. However, as we shall show, this cannot be the case. It is still true that the stress field within plastic regions must consist of a combination of centered fan and constant stress sectors, but we find that there must be a

sector of elastic unloading between the fan and the trailing constant stress region as shown in fig. 1d. The details of the analysis are complicated and, since our emphasis here is on the interpretation of results in terms of stable crack growth, we report them separately [2], outlining here only the major ideas and results.

First, RS have presented the form of the velocity field in a centered fan stress field, of type in eq. (9), which moves with the crack. This is obtained by integration of the  $rr$  and  $\theta\theta$  components of (6), noting that  $s_{rr} = s_{\theta\theta} = 0$  in a fan zone. For example, if  $a$  is crack length and the fan begins at  $\theta = \pi/4$  as in figs. 1c and d (it cannot begin at any smaller angle, nor at any larger angle, if the angular sector ahead of the tip is to be plastic, this due to the requirement of continuous shear stress), then [1] as  $r \rightarrow 0$

$$v_r = \frac{2(2-\nu)}{\sqrt{3}} \frac{\sigma_o}{E} \dot{a} \sin\theta \ln\left(\frac{\bar{R}}{r}\right) + f'(\theta) \tag{10}$$

$$v_\theta = - \frac{2(2-\nu)}{\sqrt{3}} \frac{\sigma_o}{E} \dot{a} \left( \frac{1}{\sqrt{2}} - \cos\theta \right) \left[ \ln\left(\frac{\bar{R}}{r}\right) - \frac{3\nu}{2-\nu} \right] - f(\theta) + g(r)$$

where the functions  $f(\theta)$  and  $g(r)$ , and length  $\bar{R}$ , are undetermined by the asymptotic analysis, except that  $g(0) = 0$ . The functions  $f$  and  $g$ , in addition to being functions of  $\theta$  and  $r$ , respectively, will be homogeneous functions of degree one (and possibly linear) in  $\dot{a}$  and in the rate of whatever parameter describes the intensity of the applied load. One may compute the components of  $D_{ij}$  and, since the  $D_{ij}^e$  are known in terms of  $\dot{\sigma}_{ij}$ , of  $D_{ij}^p$ . The only non-vanishing component of  $D_{ij}^p$  referred to the

polar coordinate system is, as  $r \rightarrow 0$ ,

$$D_{r\theta}^P = \frac{2-\nu}{\sqrt{6}} \frac{\sigma_o}{E} \frac{\dot{a}}{r} \ln\left(\frac{\bar{R}}{r}\right) + \frac{f''(\theta) + f(\theta)}{2r} \quad (11)$$

[Observe that since the rate quantities are referred to a moving polar coordinate system, one cannot write  $v_r = du_r/dt$ ,  $D_{r\theta} = d\epsilon_{r\theta}/dt$ , etc., although similar equations are valid for Cartesian components.]

Owing to the path-dependence (in strain space) of plastic stress-strain relations, the nature of the near tip displacement and strain field is fundamentally different for a stationary versus a growing crack. For the stationary crack,  $\dot{a} = 0$ , under monotonic load increase the only non-vanishing plastic strain in the fan is  $\epsilon_{r\theta}^P$  and this is given by an expression of the form

$$\epsilon_{r\theta}^P = F(\theta)/r, \text{ as } r \rightarrow 0, \quad (12)$$

where  $F(\theta)$  is undetermined by the asymptotic analysis. Further, the displacements at  $r = 0$  vary with  $\theta$  in the fan so that a discrete opening displacement results at the tip (the field on the size scale of this opening must be determined by a finite strain analysis). But when the crack length  $a$  is increasing continuously with the level of applied loading, asymptotic integration of eq. (11) in the manner described by Rice [10] (in the fan) and including the strain discontinuously accumulated by the velocity discontinuity at the leading edge of the fan leads to [2]

$$\epsilon_{ij}^P = \frac{2-\nu}{\sqrt{6}} \frac{\sigma_o}{E} G_{ij}(\theta) \ln\left(\frac{\bar{R}}{r}\right) + H_{ij}(\theta), \text{ as } r \rightarrow 0, \quad (13)$$

where, referred to Cartesian coordinates as in figs. 1c and d,

$$\begin{aligned} G_{xx}(\theta) &= -G_{yy}(\theta) = -2 \sin\theta \\ G_{xy}(\theta) &= G_{yx}(\theta) = \ln[\tan(\theta/2)/\tan(\pi/8)] \\ &+ 2 (\cos\theta - 1/\sqrt{2}) , \end{aligned} \tag{14}$$

and where the functions  $H_{ij}(\theta)$  are undetermined by the analysis but will depend, in a presumably monotonically increasing manner, on the ratio  $d(\text{applied load})/da$ . Further, for the growing crack the displacements in the fan vanish at  $r = 0$  and hence there is no discrete tip opening displacement.

Now, the difficulty with assuming the full Prandtl field of fig. 1c for the growing crack is that there is a non-removable discontinuity of velocity  $v_r$  at the boundary between the fan C and back constant stress zone B. Such discontinuities are permissible within an ideally plastic model, but only if they correspond to positive plastic work. Such is not the case here because, from eq. (10),  $v_r \rightarrow +\infty$  as  $r \rightarrow 0$  along the fan side and  $v_r$  is necessarily bounded along the constant stress side. Since  $\sigma_{r\theta}$  is positive, it does negative work on this discontinuity.

Several possible remedies were explored [2]. One could try to continue the field beyond the back boundary of C, in fig. 1c, by assuming an elastic zone throughout B and enforcing full continuity of velocities at the back boundary, but it is then found impossible to find a solution which does not violate yield and which meets crack surface boundary conditions. It was therefore attempted to terminate the fan at some initially unknown angle  $\theta_1$ , as shown in fig. 1d, necessarily bordering on an elastic sector, and to admit the possibility that there may be a trailing plastic region B as shown in fig. 1d, necessarily a constant state region. Alternatively, it is easily shown

that a plastic region B must exist, in the sense that the entire region  $\theta > \theta_1$  cannot be elastic, since by eqs. (13,14) material points emerge from the fan with a negatively infinite  $\epsilon_{xx}^p$  as  $r \rightarrow 0$ , requiring further yield to avoid unbounded "residual" stresses. The full details are given in [2] where it is found, for  $\nu = 0.3$ , that

$$\theta_1 \approx 115^\circ, \quad \theta_2 \approx 163^\circ \quad (15)$$

and fig. 1d has been drawn to correspond to these angles. The corresponding angles are approximately  $112^\circ$  and  $162^\circ$  for  $\nu = 0.5$ .

The resulting Cartesian stress components  $\sigma_{xx}(\theta)$ ,  $\sigma_{yy}(\theta)$ ,  $\sigma_{xy}(\theta)$  are plotted in fig. 2 for this field and for the full Prandtl field of fig. 1c. What is remarkable is how little they differ,  $\sigma_{yy}$  and  $\sigma_{xy}$  being barely distinguishable from the Prandtl values (the maximum value of  $\sigma_{yy}$ , occurring in the front constant stress sector F, is approximately 1% less than the Prandtl value of  $(2+\pi)\sigma_0/\sqrt{3}$ ), and  $\sigma_{xx}$  showing only a slight dip below the Prandtl value in the elastic sector. Presumably, this closeness has obscured the differences between the actual and the Prandtl fields for a growing crack in previous numerical simulations [1,3,4] where, to the accuracy expectable of such methods, the results were interpreted as verifying the presence of the Prandtl field.

The form of the crack opening rate  $\dot{\delta}$  (here  $\delta$  is the opening between upper and lower crack surfaces) very near the tip has also been obtained in [2]. The result has the same form as in RS, namely,

$$\dot{\delta} = \beta \frac{\sigma_0}{E} \dot{a} \ln\left(\frac{\bar{R}}{r}\right) + \dot{A}, \quad \text{as } r \rightarrow 0, \quad (16)$$

where

$$\beta = 5.083 \quad \text{for } \nu = 0.3 . \quad (17)$$

The value is  $\beta = 4.385$  for  $\nu = 0.5$  . (In RS, the value  $\beta = 4(2-\nu)/\sqrt{3} = 3.93$ , for  $\nu = 0.3$  , was obtained based on the analysis of velocities within the unapplicable full Prandtl field of fig. 1c), and where  $\dot{A}$  is undetermined by the asymptotic analysis but is homogeneous of degree one in  $\dot{a}$  and in the rate of applied load increase. Indeed, for rates of applied load which do not finitely change the elastic-plastic boundary (e.g., a negative load rate, inducing elastic response in large portions of the previously plastic zone), we expect  $\dot{A}$  to be linear in  $\dot{a}$  and the load rate. Any convenient parameter may be used to measure the applied load and, without loss of generality, we may use the far-field value of the J integral, noting that it is well-defined for contained yielding (and may be essentially so for some general yielding cases) since the far-field is elastic, and that our use of J in this case carries no implication that it is path-independent or has any meaning whatever in the near-tip plastic region. Accordingly, we write

$$\dot{A} = \alpha \dot{J}/\sigma_0 + \mu \dot{a} , \quad (18)$$

with  $\alpha$  and  $\mu$  undetermined by the asymptotic analysis, and then absorb  $\mu$  into the first term of eq. (16) to write, finally,

$$\dot{\delta} = \alpha \frac{\dot{J}}{\sigma_0} + \beta \frac{\sigma_0}{E} \dot{a} \ln \left( \frac{\bar{R}}{r} \right) , \quad \text{as } r \rightarrow 0 , \quad (19)$$

where now  $\bar{R}$  has been replaced by a new length parameter  $R$  , also undetermined



by the asymptotic analysis. In the next section we discuss the approximate determination of  $\alpha$  and  $R$ , by fitting numerical results from finite element studies [4] to the theoretical results.

It is of interest to compare near tip crack openings for stationary versus growing cracks. Setting  $\dot{a} = 0$  in eq. (19), we obtain for monotonic loading of a stationary crack

$$(\delta)_{r=0} = \int \alpha dJ/\sigma_0 = \alpha J/\sigma_0 \quad \text{for } \alpha \text{ constant} . \quad (20)$$

(Note that by dimensional analysis  $\alpha$  is constant in the small scale yielding limit; it is thought to be approximately constant up to the general yielding range for geometries such as a deeply-cracked bend specimen).

But when the crack is growing so that  $a$  increases continuously with  $J$ , asymptotic integration of eq. (19) in the manner of RS yields

$$\delta = \frac{\alpha r}{\sigma_0} \frac{dJ}{da} + \beta r \frac{\sigma_0}{E} \ln\left(\frac{eR}{r}\right) , \quad \text{as } r \rightarrow 0 , \quad (21)$$

where  $e$  is the natural logarithm base. We see that  $\delta = 0$  at the tip, but a well-defined crack tip opening angle does not exist since  $d\delta/dr \rightarrow \infty$  at  $r = 0$ .

With future discussion in mind, we may rewrite this expression as

$$\frac{E\delta}{\beta\sigma_0 R} = \left[ \frac{\alpha}{\beta} T + \ln\left(\frac{eR}{r}\right) \right] \frac{r}{R} \quad (22)$$

where  $T = (E/\sigma_0^2)dJ/da$  is the Paris tearing modulus. Now, as will be seen in the next section, and as is suggested in RS,  $R$  is found to be comparable

in size to the maximum plastic zone radius, at least under small scale yielding conditions, and  $\alpha/\beta$  is of the order 0.1. Hence in high  $T$  materials, where  $0.1 T$  greatly exceeds the logarithmic term everywhere except for values of  $r$  that are minute fractions of the plastic zone dimension, the near tip crack opening is almost linear in  $r$  and the concept of a crack opening angle has approximate validity. For example, if  $T = 200$  (in the range of reported values [5] for the more ductile structural metals) the term  $0.1 T$  is more than 5 times the logarithmic term for all values of  $r$  greater than approximately 5% of the maximum plastic zone radius. At the other end of the ductility spectrum, say  $T = 20$ , the logarithmic term exceeds  $0.1 T$  out to distances  $r$  of approximately 40% of the plastic zone radius (probably beyond the range of validity of the asymptotic result) and no meaningful definition of an opening angle could be given.

For purposes of illustration, we compare near-tip crack opening profiles in fig. 3 for a stationary crack and for growing cracks with various values of  $T$ , taking for simplicity  $\alpha = 0.65$ ,  $\beta = 5$ , and  $R = 0.2 EJ/\sigma_0^2$  (close to the value estimated in the next section for small scale yielding), so that the left side of eq. (22) is just  $\delta/(J/\sigma_0)$ . Hence, fig. 3 compares, approximately, the near tip profiles which would result at a given  $J$  level under small scale yielding. The curve marked  $T = 0$  might be thought of as a crack growing under environmental influences with negligible change in  $J$ .

### Comparison with Finite Element Results for Growing Cracks

In RS an attempt was made to identify the parameters  $\alpha$  and  $R$  appearing in eqs. (19,20) for the crack opening, by correlating the theoretical result against a finite element solution by Sorensen [3] for plane strain crack growth under small scale yielding conditions. It was remarked in RS that a numerical solution with a much finer mesh would be needed to determine more definitively the above parameters. But the tentative conclusions were reached that  $R$  scales approximately with the size of the plastic zone and that  $\alpha$  is approximately the same for a growing crack as for monotonic loading of a stationary crack. Further, two attempts were made in RS to check the theoretical  $\beta$  value against values inferred from the numerical results. Both inferred values were too large compared to what was then thought to be the theoretical value (3.93, for  $\nu = 0.3$ ). However, as remarked, the true value of  $\beta$  based on the field of fig. 1d is found to be 5.08 for  $\nu = 0.3$ , and this is not far from the inferred value of 4.8 in RS, based on displacement increments at the second node back from the tip.

A refined mesh finite element solution of the kind advocated in RS has now been carried out by Sham [4]. We discuss some of the results here. The formulation of the small scale yielding problem, type of elements used, and general features of the mesh layout are in all respects similar to those of [3] except the mesh is finer, so that the plastic zone size in the range for which crack growth is studied is of the order 50 times the side length of the smallest elements. These smallest elements are of uniform size along and adjacent to the path of crack growth, and consist of squares laid out in a rectangular array, with each square made up of 4 constant-strain triangular finite elements sharing a common node at its center. The material is an ideally plastic Mises solid with  $\nu = 0.3$  and the loading, as appropriate

for small scale yielding, is specified in terms of the far field Mode I stress intensity factor  $K$ . Some of Sham's results will be reported in terms of  $J$ , where it is to be understood that  $J$  has the "far-field" value appropriate for contours in the elastic region, namely  $(1-\nu^2)K^2/E$ .

The load versus crack length history is shown in the inset diagram in fig. 4, where  $K_0$  is the load required to yield the first element. The load is first increased without crack growth to slightly below  $10 K_0$ , then 3 one-element crack growth steps are simulated (by incremental unloading of crack tip nodes at fixed  $K$ ), each followed by an increase in  $K$  at fixed crack length, and then 8 further one-element crack growth steps are simulated at fixed  $K$ .

Sham [4] reported the near tip stress fields for both the stationary and growing crack cases to be consistent with the full Prandtl field of fig. 1c. But as shown in fig. 2, the differences between the full Prandtl field and its modification with the elastic sector of fig. 1d are small. The numerical results for stresses are not accurate enough (presumably because they are based on a mesh with non-singular elements at the tip; compare [12]) to distinguish between the two, and can equally be regarded as being consistent with the field associated with fig. 1d for the growing crack. Nevertheless, Sham reports that all crack growth steps are accompanied by elastic unloading of some elements behind the tip, of locations coinciding roughly with the location of the elastic sector in fig. 1d. Further, elements adjoining the crack surfaces near the tip are found to yield in a direction corresponding to extension in the  $x$ -direction of fig. 1d, as predicted within region B, and which is expected since material points emerge from the fan with a value of  $\epsilon_{xx}^P$  which becomes negatively infinite at the tip. Thus these features as well as the element stresses near the tip are consistent with the theoretical analysis [2] of the field at a growing crack tip.

For small load increase at fixed crack length, eq. (19) suggests a variation  $\Delta\delta$  in crack tip opening displacement given by

$$(\Delta\delta)_{r=0} = \alpha \Delta J/\sigma_0 . \quad (23)$$

Thus we are able to estimate the dependence of  $\alpha$  on the amount of crack growth by estimating  $(\Delta\delta)_{r=0}$  from the numerical results for the various load increases at fixed crack length shown in fig. 4. This is accomplished in fig. 4a for the three load steps following growth, by plotting  $\Delta\delta/(\Delta J/\sigma_0)$  at the crackline nodes as a function of  $r/(K/\sigma_0)^2$ . The results suggest that at least for the rather modest amounts of crack growth considered, the incremental openings for load increase at fixed crack length are unaffected by growth; i.e., that  $\alpha$  is essentially constant during growth. To determine the relation between  $\delta$  and  $J$  for monotonic loading of a stationary crack, we observe that by dimensional considerations  $\alpha$  is constant during monotonic loading under small scale yielding conditions, but that its value is most accurately estimated from numerical solutions by using data from the range in which the plastic zone size is large compared to element size. Accordingly, in fig. 4b we show  $\Delta\delta/(\Delta J/\sigma_0)$  versus  $r/(K/\sigma_0)^2$  from data based on the last few increments of loading of the stationary crack, as indicated.

The points of figs. 4a and b superpose on one another everywhere except in the region of upturn. If the upturn region is ignored and the data is extrapolated to the tip, as shown by the dashed line, we obtain  $\Delta\delta/(\Delta J/\sigma_0) = 0.53$  in both cases, i.e.,  $\alpha = 0.53$ , the value being the same for both the stationary and growing crack. This value of  $\alpha$  is somewhat smaller than the

accepted value of approximately 0.65 for the stationary crack (see RS for a summary of results), whereas  $\alpha \approx 0.65$  is consistent with the opening at the first node back from the tip in fig. 4b. If we use similarly the opening at the first node in fig. 4a to estimate  $\alpha$  for the growing crack, then the values of  $\alpha$  are higher (0.69, 0.71, 0.72 at the end of the three growth steps) than for the stationary crack, i.e., by amounts ranging from 6% to 11%. The interpretation of these results is further clouded by the upturns in  $\Delta\delta$ , which occur within a region for which the finite element mesh of [4] undergoes a reduction by a factor of 2 in element size (starting 3 elements behind the original crack tip), and may indicate inadequacies of the numerical treatment.

The last 8 one-element steps of growth (release steps 4 to 11) at fixed  $K$  grow the crack away from the region of discontinuity in mesh size. Observing from eq. (21) that for growth at constant  $K$  (hence constant  $J$ ) the near tip opening is

$$\delta = \beta \frac{\sigma_o}{E} r \ln\left(\frac{eR}{r}\right), \quad (24)$$

comparison of the finite element results for  $\delta$  with this formula provides a means of estimating  $R$  and of seeing to what extent the numerical results are consistent with the theoretical value of  $\beta$ . To do so, the formula is rewritten as

$$\frac{E\delta}{\sigma_o r} = \beta \ln\left[\frac{R}{(K/\sigma_o)^2}\right] + \beta \ln\left[\frac{e(K/\sigma_o)^2}{r}\right] \quad (25)$$

and  $E\delta/\sigma_o r$  is plotted against  $\ln[e(K/\sigma_o)^2/r]$ , so that  $\beta$  is given by the

slope and  $R$  is determined from the axis intercept. This is done in fig. 5 for the finite element openings along the path of growth at constant  $K$ , using data at the end of each of the release steps 6 to 11. The data for each release step forms a straight line, confirming the logarithmic dependence in eq. (24), and the slopes are very close to one another;  $\beta = 5.4$  can be taken as a representative value. This is close to, but somewhat larger than, the theoretical value of 5.08. The corresponding values of  $R$  as determined from axis intercepts are shown in fig. 5, and these cluster about the value

$$R \approx 0.21 K^2/\sigma_0^2 \approx 0.23 EJ/\sigma_0^2, \quad (26)$$

which seems to be essentially independent of the amount of growth. Further, Sham [4] estimates a maximum plastic zone radius which is approximately  $0.16 (K/\sigma_0)^2$  for the stationary crack and which increases slightly with growth, to approximately  $0.18 (K/\sigma_0)^2$  at the end of the 11 growth steps. Thus the value estimated above for  $R$  essentially scales with the plastic zone size but is about 15% to 30% larger.

Again, however, the interpretation of numerical results is not unambiguous. For example, if lines with the theoretical slope  $\beta = 5.08$  are fit to the data of fig. 5, the value of  $R$  is found to decrease with crack growth, from  $R \approx 0.35 (K/\sigma_0)^2$  at release step 6 to  $R \approx 0.21 (K/\sigma_0)^2$  at release step 11.

Clearly, much remains to be done to determine expressions for the parameters  $\alpha$  and  $R$  and for their dependence on crack growth, not only for the small scale yielding case examined here but also for larger scale yielding. Lacking more definitive information, we will assume tentatively for the subsequent discussion of crack growth that  $\alpha$  is approximately constant and that  $R$  scales with the plastic zone size (in the form  $R \approx 0.2 EJ/\sigma_0^2$  for small scale yielding).

Speculations on Large Scale Yielding

The numerical results just surveyed, as well as those in the original RS study, were for the small scale yielding limit, in which the plastic response is fully determined by the surrounding elastic  $K$  field. However, the results of the asymptotic analysis should be valid for larger scale contained yielding of ideally plastic solids, although  $R$  and  $\alpha$  must then be expected to depend on the extent of yielding. For example, the tentative relation  $R \approx 0.2 EJ/\sigma_0^2$  cannot be expected to persist at large scale yielding because the dimensions of the plastic region no longer scale directly with  $J$ .

Finally, for fully yielded ideally plastic specimens, of a geometry that retains constraint comparable to that of the Prandtl field (e.g., deeply-cracked bend specimens [15]), growth of the crack still requires that centered fan sectors of near tip stresses be moved through the material. This introduces logarithmic singularities of the type multiplying  $\dot{a}$  in expressions like those of eqs. (10) for the near tip velocities, and leads, ultimately, to an expression in the form of eq. (16) for the near tip opening rates, namely

$$\dot{\delta} = \beta \frac{\sigma_0}{E} \dot{a} \ln \left( \frac{\bar{R}}{r} \right) + \dot{A}, \quad \text{as } r \rightarrow 0.$$

For a geometry like that of the tensile specimen with deep double edge cracks, for which the full Prandtl field provides the near tip state for the stationary crack case, the construction of fig. 1d is expected to apply during growth so that  $\beta$  has the same value as given earlier, eq. (17). For a geometry like that of the deeply-cracked bend specimen, the stress field for a stationary crack is very close to that of the full Prandtl field [15], and hence a similar value of  $\beta$  is expected in that case (we leave open the question of whether the value would be identical).



Regardless of the extent of yielding,  $\dot{A}$  in eq. (16) will be homogeneous of degree one in  $\dot{a}$  and in some loading parameter such as the imposed displacement (say,  $q$ ) at the load point. For reasons discussed earlier, we believe it may be appropriate to regard the dependence as being linear in  $\dot{a}$  and  $\dot{q}$ , say

$$\dot{A} = \xi \dot{q} + \bar{\mu} \dot{a}$$

where  $\xi$  and  $\bar{\mu}$  are parameters undetermined by the asymptotic analysis. Now, suppose a quantity  $J$ , to be associated in an as yet imprecise way with the  $J$  integral, is defined in some way, for all extents of yielding, such that  $\dot{J}$  is linear in  $\dot{q}$  and  $\dot{a}$ . Then we can write, analogously to eq. (18),

$$\dot{A} = \alpha \dot{J} / \sigma_0 + \mu \dot{a}$$

where, again,  $\alpha$  and  $\mu$  are undetermined by the asymptotic analysis. In the Appendix we discuss two different ways of defining  $J$ : one ( $J_f$ ) based on a far field contour; another ( $J_d$ ) based on a "deformation theory" definition, i.e.,  $J_d$  is the same function of  $a$  and  $q$  as for monotonic loading to  $q$  with  $a$  fixed. Different definitions of  $J$  will lead to different values of  $\mu$  (and perhaps  $\alpha$ ). Thus, when we follow the steps from eqs. (16) and (18) to eqs. (19), (20) and (21), which are now seen to apply to all extents of yielding, it must be recognized that  $R$  will depend on the way that  $J$  is defined, since it incorporates the  $\mu \dot{a}$  part of the expression for  $\dot{A}$ .

To apply dimensional considerations in order to understand the behavior of  $R$ , say, as a function of  $J$ , it is now necessary to be more precise about the definition of  $J$  at large scale yielding. In particular, in the limit of a fully yielded specimen of rigid-ideally plastic material, it is obvious

that  $\dot{\delta}$  at the tip must take the form  $\dot{\delta} = \omega \dot{q}$  where  $\omega$  is some parameter (possibly dependent on the geometry of the cracked body) and, further, we observe that for rigid-plastic materials this expression for  $\dot{\delta}$  is equally valid for stationary or for growing cracks (i.e., it is independent of  $\dot{a}$ ). Now, if  $R$  is to remain well defined in the rigid-plastic limit, as  $\sigma_0/E \rightarrow 0$ , it is necessary that whatever expression we adopt for  $J$  be such that in this limit  $\dot{J}$  depends only on  $\dot{q}$  and not on  $\dot{a}$ . Otherwise the term  $R$  in eq. (19) would have to contain a factor  $\exp[(\text{constant}) \times E/\sigma_0]$  to cancel out the  $\sigma_0/E$  in front of the  $\ln$  term of (19), and thus annul the  $\dot{a}$  dependence of  $\dot{J}$ , as  $\sigma_0/E \rightarrow 0$ . We show in the Appendix, for the rigid-plastic bend specimen, that  $J_f$ , the value of the  $J$  integral associated with an appropriate far field contour, has this property, whereas  $J_d$  does not. We do not, however, suggest that  $J_f$  will have this property for all specimen geometries and, indeed, we find that  $J_d$  has the appropriate property in the case of a tension specimen with deep double edge cracks.

With the understanding that  $J$  has been appropriately defined so that  $R$  has no spurious dependence on a term like  $\exp[(\text{const.}) \times E/\sigma_0]$ , we now observe that the terms containing  $R$  in eqs. (19,21) arise from moving a centered fan stress distribution through an elastic-plastic material. Thus  $R$  should scale approximately with the size of the region over which such fan-like stress fields prevail. Hence, with reference to the deeply-cracked bend specimen of fig. 6,  $R$  should saturate in size to some fraction of the ligament dimension  $b$  as fully plastic conditions are attained. Hence, as shown in fig. 6, we expect  $R$  to increase linearly with  $J$  at first, as appropriate to the small scale yielding regime, but then to saturate as  $J$  further increases. The saturation level of  $R \approx b/4$  is only a guess and

much further correlation of the asymptotic analysis against numerical results will be necessary to establish this level and, indeed, the full dependence of  $R$  on  $J$ .

There is, of course, already an approximation built into the notion that  $R$  should depend on  $J$  (and, of course, on geometric dimensions such as crack depth and ligament size):  $R$  should have at least some dependence on the amount of prior crack growth. However, as suggested by results for small scale yielding, this dependence seems to be minor, probably because the shape and size of the currently active plastic zone is not strongly affected by prior growth. The point needs further clarification, but is neglected in our subsequent discussion of crack growth criteria.

### Investigation of a Ductile Crack Growth Criterion

Here we investigate implications of the ductile crack growth criterion proposed in RS. This is based on the opening  $\delta$  at a small characteristic distance from the tip, but, as will be seen, the criterion is similar in form to other criteria which might be proposed based on other parameters of the near tip deformation field, e.g., on local plastic strain.

It is important to remember, however, that the criterion is based on the deformation field, and makes no reference to the stress distribution. Such might be considered reasonable in the sense that the maximum tension immediately at the crack tip is always essentially the same (equal to the Prandtl value or a percent or so lower) for the highly constrained geometries that we consider, so that the only variable features of the near tip field are the levels of strain and opening displacement. But it is possible that the critical levels of deformation could, in some cases, be influenced by the "pre-conditioning" (e.g., microcrack or cavity nucleation) of material elements by high stress levels experienced before the crack arrives. This pre-conditioning could be more severe when the region of triaxially elevated stresses extends over larger versus smaller size scales ahead of the crack. On the other hand, for cases of ductile rupture in which cavity nucleation is limited to the immediate vicinity of the crack tip (say, over a size scale comparable to the tip opening displacement for a stationary crack), the size scale over which the triaxially elevated stress state extends ahead of the crack is expected to be unimportant, and a growth criterion based on local deformations seems appropriate.

The model criterion of RS assumes that growth initiates by large plastic strains associated with opening at the stationary crack tip, and that once growth has thereby occurred over a distance comparable to the fracture process

zone, subsequent growth continues in a mode for which a geometrically similar (in a sense to be made precise) profile of crack opening is maintained very near the tip. Now, the equation for the near tip profile, eq. (21), does not admit a solution with non-zero  $dJ/da$  in which  $\delta$ , as a function of  $r$ , is strictly similar. Therefore, the criterion for growth is stated in RS as the requirement (fig. 7) that a critical opening  $\delta = \delta_c$  be maintained at a small characteristic distance  $r_m$  (called  $\Delta l$  in RS) behind the tip. Thus, from eq. (21), the criterion for continuing crack growth is that

$$\frac{\delta_c}{r_m} = \frac{\alpha}{\sigma_o} \frac{dJ}{da} + \beta \frac{\sigma_o}{E} \ln \left( \frac{eR}{r_m} \right) \quad (27)$$

Since  $R$  is regarded as a function of  $J$  (though specimen dependent; i.e., dependent also on  $a$ , at large scale yielding (fig. 6)), eq. (27) can be regarded as a first order differential equation which determines the manner in which  $J$  must vary with  $a$  in order to continue to meet the crack growth criterion. The initial condition is that  $J = J_{IC}$  (the initiation value) at  $a = a_o$  (the initial crack length).

It seems appropriate to regard  $r_m$  as a size comparable to that of the "fracture process zone," although this is, of course, not a sharply-defined size. It is tempting to identify  $\delta_c$  with the crack tip opening displacement,  $\delta_{IC} = \alpha J_{IC} / \sigma_o$ , at the onset of growth, but experimental observations are well known to reveal crack profiles during growth that suggest much less near tip opening than at initiation. Thus  $\delta_c$  is regarded as an independent empirical parameter, sometimes much smaller than  $\delta_{IC}$ . Indeed, as discussed in RS,  $\delta_{IC}$  might more sensibly be regarded as a measure of the fracture process zone

size, and hence of  $r_m$ .

Now, the solutions to eq. (27) show the manner in which  $J$  must vary with  $a$ , beyond the  $J_{IC}$  point, to meet the crack growth criterion. In some cases, e.g., sufficiently low  $\delta_c/r_m$  and high  $\sigma_o/E$ , it may happen that the value of  $dJ/da$  calculated from eq. (27) at the  $J_{IC}$  point is negative. In such cases, immediately unstable crack growth is expected. For more ductile materials (i.e., sufficiently large  $\delta_c/r_m$  and small  $\sigma_o/E$ ), the calculated  $dJ/da$  is positive and integration of the equation leads to a  $J$  vs.  $a-a_o$  relation which must be followed for stable growth. It may happen, however, that the predicted  $dJ/da$  at some point in the growth history falls below what the loading system can supply, and at that point unstable crack growth occurs. Specifically, let  $J_A(Q,a)$  be the "applied"  $J$  where  $Q$  is a monotonically increasing measure of the intensity of loading. In different cases  $Q$  may represent an imposed force or stress, or an imposed load-point displacement (or a displacement imposed on a compliant loading system attached to the cracked body). Then, if  $J(a)$  represents the solution of eq. (27) for the given cracked body and initial conditions ( $J = J_{IC}$  when  $a = a_o$ ), the variation of  $Q$  with  $a$  satisfies

$$J_A(Q,a) = J(a) \tag{28}$$

and instability ( $dQ/da \rightarrow 0$ ) occurs when, simultaneously, this equation and

$$\partial J_A(Q,a)/\partial a = dJ(a)/da \tag{29}$$

are met. These equations have a well-known graphical solution in terms of tangential contact of the curves  $J = J(a)$  and  $J = J_A(Q,a)$ , for fixed  $Q$ ,

on a  $J$  versus  $a$  diagram, although our work carries no implication that the "resistance" curve  $J(a)$  is invariant to specimen geometry at large scale yielding.

For crack growth under small scale yielding we can write

$$R = \lambda EJ/\sigma_o^2 \quad \text{where, eq. (26), } \lambda \approx 0.2, \quad (30)$$

and thus (27) becomes

$$\frac{\alpha}{\sigma_o} \frac{dJ}{da} = \frac{\delta_c}{r_m} - \beta \frac{\sigma_o}{E} \ln \left( \frac{e\lambda EJ}{r_m \sigma_o^2} \right) \quad (31)$$

We present the integrals of this equation in a somewhat different way than RS, rewriting it as

$$T \equiv \frac{E}{\sigma_o^2} \frac{dJ}{da} = T_o - \frac{\beta}{\alpha} \ln \left( \frac{J}{J_{IC}} \right) \quad (32)$$

Here  $T_o$  is the value of the Paris tearing modulus at the onset of growth under small scale yielding conditions, and is given by

$$T_o = \frac{E}{\alpha \sigma_o} \frac{\delta_c}{r_m} - \frac{\beta}{\alpha} \ln \left( \frac{e\lambda EJ_{IC}}{r_m \sigma_o^2} \right), \quad (33)$$

where  $\alpha$  has the value appropriate to small scale yielding ( $\approx 0.65$ ). In fact, it is possible to express the crack growth criterion at all levels of yielding, whether small scale or not, in terms of the two macroscopic parameters  $J_{IC}$  and  $T_o$ ; there is no need to measure directly the microscale parameters  $r_m$

and  $\delta_c/r_m$ . The integrals of eq. (32) for small scale yielding are shown in fig. 8 where we have set  $\alpha = 0.65$ ,  $\beta = 5.08$  and plotted

$$J/J_{IC} \text{ versus } (a-a_0)/[0.2EJ_{IC}/\sigma_0^2]$$

for a range of values of  $T_0$ . Here the crack growth  $(a-a_0)$  has been made dimensionless by a quantity which is equal approximately to the maximum radius of the plastic zone at the onset of growth. All the curves in fig. 8 exhibit a plateau, corresponding to steady state growth (i.e.,  $dJ/da \rightarrow 0$ ), at  $J$  levels given by

$$J_{ss} = J_{IC} \exp(\alpha T_0/\beta) = J_{IC} \exp(0.128 T_0) . \quad (34)$$

For materials with large  $T_0$  values, say  $T_0 > 25$ , this level is so large (e.g.,  $J_{ss} > 25 J_{IC}$ ) that in cracked bodies of practical sizes, large scale and, finally, fully plastic yielding conditions will occur well before  $J$  approaches  $J_{ss}$ , invalidating the calculation. Of course, even for crack growth under small scale yielding, the instability condition of eqs. (28,29) will usually be met before  $J$  reaches  $J_{ss}$ .

More generally, at large scale yielding, the crack growth criterion of eq. (27) may be put in the form

$$T \equiv \frac{E}{\sigma_0^2} \frac{dJ}{da} = \frac{\alpha_{ssy}}{\alpha} T_0 - \frac{\beta}{\alpha} \ln \left( \frac{R}{\lambda E J_{IC} / \sigma_0^2} \right) \quad (35)$$

where now  $\alpha_{ssy} \approx 0.65$  represents the small scale yielding value of  $\alpha$  and we admit the possibility that  $\alpha \neq \alpha_{ssy}$  at large scale yielding. Here  $R = \lambda E J_{IC} / \sigma_0^2$  at small scale yielding but (fig. 6) deviates from this at larger



scale yielding and finally saturates in value at fully yielded conditions. The argument of the  $\ln$  term is the ratio of  $R$  to the value which it would have at the onset of growth under small scale yielding conditions. It is this  $\ln$  term which exhibits the sensitivity of the growth criterion at full plasticity to specimen size. For example, taking the numerical values of  $\beta$  and  $\alpha_{ssy}$  as above, setting  $\lambda = 0.2$  as suggested in eq. (30), and guessing as in fig. 6 that the saturation value of  $R$  is approximately  $b/4$ , we have at fully yielded conditions

$$T \equiv \frac{E}{\sigma_o^2} \frac{dJ}{da} \approx \left[ T_o - 7.8 \ln \left( \frac{b/4}{0.2EJ_{IC}/\sigma_o^2} \right) \right] \frac{\alpha_{ssy}}{\alpha_{fy}} \quad (36)$$

$$\approx 1.3 T_o - 10.0 \ln \left( \frac{b/4}{0.2EJ_{IC}/\sigma_o^2} \right)$$

for the bend specimen, where we have taken  $\alpha_{fy}$  (the value of  $\alpha$  for fully yielded conditions) as 0.51 in the last version, so that  $\alpha_{ssy}/\alpha_{fy} \approx 1.3$ . This value of  $\alpha_{fy}$  is suggested by the rigid-plastic solution (see Appendix); the actual  $\alpha_{fy}$  for growth in an elastic-plastic material may be less different from  $\alpha_{ssy}$ .

Two observations can be made. First, if crack growth begins under fully yielded conditions the growth curve  $J$  versus  $a-a_o$  (according to the ideally plastic model and other assumptions that we have made) is qualitatively different from that for small scale yielding.  $T$  is then essentially constant for amounts of growth that are small compared to ligament size (so that  $b$  in

eq. (36) does not change significantly) and, if the formula is regarded as being accurate for large amounts of growth,  $T$  actually is predicted to increase with  $a-a_0$  (since  $b$  diminishes), in marked contrast to the small scale yielding behavior in fig. 8.

Second, the (essentially constant) value of  $T$  for small, fully plastic growth will not be identical to  $T_0$ . The difference between the two arises in part because of the ratio  $\alpha_{ssy}/\alpha_{fy}$  in (36). If this ratio were near to unity (as it seems to be for the deeply double edge-cracked tensile specimen; see Appendix), then the difference between  $T$  and  $T_0$  would generally be negligible for high  $T_0$  materials, since the argument of the  $\ln$  term in eq. (36) will seldom be very small or large compared to unity in practical cases. But for low  $T_0$  materials the differences could be significant. For example, the argument of the  $\ln$  term is approximately equal to the ratio of the quarter-ligament size to the plastic zone size corresponding to onset of growth in a large specimen, sustaining small scale yielding conditions. For a specimen which is sufficiently small that  $J_{IC}$  conditions are attained only in the fully plastic regime, this ratio is expected to be less than unity, so that  $T$  exceeds  $T_0$  (or  $T_0 \alpha_{ssy}/\alpha_{fy}$  if variations in  $\alpha$  are considered).

For example, consider a material which is tested in a specimen size at the limit of what is regarded as the permissible range for a valid fully plastic  $J_{IC}$  test, namely  $b = 25 J_{IC}/\sigma_0$ . Then eq. (36) predicts

$$\begin{aligned}
 T &\approx [T_0 + 7.8 \ln(E/31\sigma_0)] \alpha_{ssy}/\alpha_{fy} \\
 &= [T_0 + 22] \alpha_{ssy}/\alpha_{fy} \approx 1.3 T_0 + 28 \quad , \quad \text{for } \sigma_0/E = 0.002 \\
 &= [T_0 + 13] \alpha_{ssy}/\alpha_{fy} \approx 1.3 T_0 + 17 \quad , \quad \text{for } \sigma_0/E = 0.006
 \end{aligned}
 \tag{37}$$

where the last expressions given for each strength level are based on  $\alpha_{ssy}/\alpha_{fy} = 1.3$ , as may be approximately correct for a bend specimen. We note that when the observed fully plastic  $T$  value is sufficiently small,  $T_0$  would have to be negative. Such a material would be expected to show immediately unstable fracture when tested in specimens that are large enough to meet small scale yielding conditions, although it exhibits stable crack growth in small, fully plastic specimens. On the other hand, if the fully plastic  $T$  value is large, say, greater than 100, the effect of the  $\ln$  term can be disregarded and differences between  $T$  and  $T_0$  arise only because (or if)  $\alpha_{fy}$  differs from  $\alpha_{ssy}$ .

In fact in this latter case of high  $T$  materials, the  $\ln$  terms in eqs. (35,36) are negligible, and hence the  $J$  versus  $a-a_0$  relation, at least for small amounts of growth, is expected to show negligible dependence on specimen size in the fully yielded range. In this respect our conclusions are in partial agreement with those of Hutchinson and Paris [6], and this is of interest because the basic assumptions are very different in the two approaches. Hutchinson and Paris appeal to strain hardening of the material (whereas we have neglected hardening) and assume that this hardening is sufficiently strong to create a HRR singular zone near a stationary crack tip, so that the near tip field is then uniquely characterized by  $J$ . Next, they consider crack growth under increasing imposed displacement on the specimen, and observe that if the imposed displacement increases rapidly enough with increasing  $a$ , effects of strongly non-proportional stressing are limited to a small neighborhood of the tip, whereas at greater distances the stress histories are such that the approximation of deformation plasticity theory is valid. Hence they assume that a far field value of  $J$  is well-defined and path-independent everywhere except very near the tip, and this assumption has confirmation from the

numerical studies of Shih [16], which are based on incremental plasticity and model observed crack growth in a high  $T$  material. Hence, for sufficiently large  $T$ , and degree of hardening, and for sufficiently limited amounts of crack growth, Hutchinson and Paris assume that the growth process takes place in a surrounding HRR singular field that is uniquely characterized by  $J$ , so that there is a universal relation of  $J$  to  $a-a_0$ . Further, their work carries the implication that this same relation would apply for small scale yielding, although our work does not support this notion, even for high  $T$  materials, when the ratio  $\alpha_{ssy}/\alpha_{fy}$  of eq. (36) differs from unity. (We also note that Hutchinson and Paris [6] tacitly assume that this far field  $J$  value, say,  $J_f$ , can be equated to the "deformation theory" function  $J_d = J_d(q,a)$ . We show in the Appendix that the two are definitely different in the rigid-plastic limit, although the differences between  $J_f$  and  $J_d$  will often be small for high  $T$  materials).

In comparison to the Hutchinson and Paris approach, our growth criterion is based on the actual structure of near tip fields as predicted for a material of the incremental plasticity type. Indeed, the near tip fields are strongly influenced by the path-dependent constitutive response of such a material. On the other hand, we have modelled the material as ideally plastic and this probably tends to overestimate dependences on the extent of yielding, particularly those arising from differences between  $\alpha_{ssy}$  and  $\alpha_{fy}$ , since, on the basis of the HRR fields, hardening is widely thought to lead to a lessened dependence of  $\alpha$  on the extent of yielding than predicted from ideally plastic solutions. Also, while it is clear that an incremental formulation of the plasticity equations is correct physically, there is reason to believe that models of the Prandtl-Reuss-Mises type, which assume invariant shapes of yield surfaces in stress space, may not be fully adequate for strongly non-proportional stress histories as experienced near a growing crack.

While it is of interest that our approach and that of Hutchinson and Paris are consistent, at least to the neglect of  $\alpha$  variations, for high T materials, it is well to remember that both approaches rest on assumptions which require more study for full understanding of their range of validity. Also, enthusiasm over this concurrence of conclusions should be tempered by the recognition that the high T materials may be so resistant to crack growth that unstable crack propagation is seldom likely to be a practical problem. On the other hand, for low T materials, which are more prone to instability, the conditions which Hutchinson and Paris state for validity of a universal J versus  $a-a_0$  relation are not met, and our work suggests significant dependencies on the extent of yielding and specimen size.

We close this section by outlining an alternate crack growth criterion based on near tip plastic straining. The centered fan velocity field of eqs. (10) includes the function  $f(\theta)$ , which is homogeneous of degree one in  $\dot{a}$  and in the rate of applied load. If, analogously to the transition from eq. (16) to (19) in the expression for  $\dot{\delta}$ , we assume this dependence to be linear in  $\dot{a}$  and the load rate, then it is straightforward to show that the asymptotic integration leading to eq. (13) for  $\epsilon_{ij}^P$  yields expressions of the form, as  $r \rightarrow 0$ ,

$$\dot{\epsilon}_{ij}^P = \frac{2-\nu}{\sqrt{6}} \frac{\sigma_0}{E} G_{ij}(\theta) \ln \left[ \frac{L_{ij}(\theta)}{r} \right] + \frac{1}{\sigma_0} M_{ij}(\theta) \frac{dJ}{da} \quad (38)$$

in the fan for a continuously growing crack (here no summation is implied by repeated indices). The functions  $G_{ij}(\theta)$  are given by eqs. (14), but the functions  $L_{ij}(\theta)$ , of length dimensions, and the dimensionless functions  $M_{ij}(\theta)$  are undetermined by the asymptotic analysis.

Similarly, the equivalent plastic shear strain  $\gamma^P$ , with rate defined by

$$\dot{\gamma}^P = \sqrt{2D_{ij}^P D_{ij}^P} = 2D_{r\theta}^P \quad \text{in the fan,} \quad (39)$$

is obtained by integration of eq. (11), adding on the  $\gamma^P$  accumulated discontinuously at the front boundary of the fan. This results in

$$\gamma^P = \frac{2(2-\nu)}{\sqrt{6}} \frac{\sigma_o}{E} \left\{ \sqrt{2} + \ln \left[ \frac{\tan(\theta/2)}{\tan(\pi/8)} \right] \right\} \ln \left[ \frac{L(\theta)}{r} \right] + \frac{M(\theta)}{\sigma_o} \frac{dJ}{da} \quad (40)$$

where the length function  $L(\theta)$  and dimensionless function  $M(\theta)$  are again undetermined by the asymptotic analysis. For example, setting  $\theta = \pi/2$ ,  $\gamma^P$  represents the equivalent shear strain accumulated in the forward part of the fan and is given by

$$\gamma^P = 1.88 (2-\nu) \frac{\sigma_o}{E} \ln \left( \frac{L}{r} \right) + \frac{M}{\sigma_o} \frac{dJ}{da}, \quad (41)$$

where  $L = L(\pi/2)$ ,  $M = M(\pi/2)$ . Although verification would require detailed comparison with numerical solutions in a region where these have great inaccuracies, it seems reasonable to expect that  $L$  scales with the size of the plastic region, being approximately proportional to  $EJ/\sigma_o^2$  for small scale yielding, and that  $M$  is approximately invariant to growth. Hence the features of the terms in this equation are expected to be similar to those of analogous terms in eq. (21).

Accordingly, if we require as a criterion for continuing crack growth that all points closer than a certain small characteristic distance  $r_m$  above and below the tip have accumulated a plastic strain equal to or greater than a critical value  $\gamma_c^P$  as the crack approaches, we obtain

$$\gamma_c^p = \frac{M}{\sigma_o} \frac{dJ}{da} + 1.88 (2-\nu) \frac{\sigma_o}{E} \ln \left( \frac{L}{r_m} \right) \quad (42)$$

as the differential equation governing growth. This is identical in form to the criterion studied here (compare eq. (27)) and is expected to lead to qualitatively similar conclusions.

Appendix: Interpretation of J at Full Plasticity

To clarify the interpretation of the term involving  $\dot{J}$  in eq. (19), and  $dJ/da$  in eq. (21), for fully plastic specimens, consider the cracked bend specimen of fig. 6 to consist of rigid-ideally plastic material. Let  $\theta$  be the rotation of one end of the specimen relative to the other. Then [10] the moment required to continue deformation is

$$M = (0.63/\sqrt{3}) \sigma_0 b^2 \quad (A-1)$$

and the rate of opening at the tip is

$$\dot{\delta} = 0.37 b \dot{\theta} . \quad (A-2)$$

These formulae are valid for stationary or growing cracks, and when the latter is integrated for a continuously growing crack we obtain, for small  $r$  ,

$$\delta = 0.37 r b d\theta/da . \quad (A-3)$$

As remarked in the text, if eqs. (19) and (21) are to reduce to (A-2) and (A-3) in the rigid plastic limit ( $\sigma_0/E \rightarrow 0$ ) with bounded  $\ln R$  , it is necessary that the definition of  $J$  be such that in this limit it reduces to an expression for which  $\dot{J}$  depends only on  $\dot{\theta}$  and not on  $\dot{a}$  .

We examine two candidate definitions of  $J$  . First, the deformation theory definition takes  $J$  to be the same function of  $\theta$  and  $a$  (or  $b$ ) as it would be if the current rotation  $\theta$  were imposed at a fixed value of  $b$  , namely the current  $b$  value. This  $J$  , called  $J_d$  , is given in the rigid-plastic



case by the well-known expression

$$J_d = \frac{2}{b} M\theta = [2(0.63)/\sqrt{3}] \sigma_o b\theta = 0.73 \sigma_o b\theta . \quad (A-4)$$

It does not have the desired feature, because

$$\dot{J}_d = 0.73 \sigma_o (b\dot{\theta} - \theta\dot{a}) . \quad (A-5)$$

An alternate definition is the far field contour  $J$ , called  $J_f$  and, for definiteness this is taken on the dashed line contour  $\Gamma_1 + \Gamma_2 + \Gamma_3$  coinciding with the specimen boundary in fig. 6. Thus

$$J_f = 2 \int_{\Gamma_1 + \Gamma_2 + \Gamma_3} (W dy - T_i \partial u_i / \partial x ds) \quad (A-6)$$

(the factor 2 appears because only one-half of a complete contour is considered),

where

$$W = \int \sigma_{ij} d\epsilon_{ij} \quad (A-7)$$

is the density of stress working,  $T_i$  the traction and  $u_i$  the displacement vector. The term with  $T_i$  vanishes on stress free surfaces  $\Gamma_1$  and  $\Gamma_3$ , and it makes no net contribution on  $\Gamma_2$  since each  $\partial u_i / \partial x$  is uniform there (the boundary is rigid) and the integrated value of each  $T_i$  on  $\Gamma_2$  vanishes since the loading is pure bending. Also,  $W$  vanishes on the rigid boundaries  $\Gamma_2$  and  $\Gamma_3$  whereas on  $\Gamma_1$  it has the value

$$W = -(2\sigma_o/\sqrt{3}) \epsilon_{yy} = -(2\sigma_o/\sqrt{3}) \partial u_y / \partial y \quad (A-8)$$

since those points along  $\Gamma_1$  which yield do so in compression under stress  $\sigma_{yy} = -(2\sigma_o/\sqrt{3})$ . Hence

$$J_f = 2 \int_{\Gamma_1} W dy = (2\sigma_o/\sqrt{3}) [-2u_y^P] \quad (A-9)$$

where  $u_y^P$  is the vertical displacement at point P in fig. 6. Now, the motion of the rigid portions of the rigid-plastic specimen is well-known to consist of rotation about a "hinge point" having an x coordinate which extends a distance 0.37 b ahead of the tip [10], and hence

$$2\dot{u}_y^P = -(b-0.37b)\dot{\theta} = -0.63b\dot{\theta} \quad (A-10)$$

Thus

$$J_f = [2(0.63)/\sqrt{3}] \sigma_o \int_0^\theta b d\theta = 0.73\sigma_o \int_0^\theta b d\theta \quad (A-11)$$

where the integral follows the history of crack growth (i.e., b will in general vary with  $\theta$ ). It is obvious that  $J_f = J_d$  of (A-4) when the crack does not grow as  $\theta$  is applied. But when the crack is growing  $J_f$  exhibits the desired feature

$$\dot{J}_f = 0.73\sigma_o b\dot{\theta} \quad (\text{i.e., independent of } \dot{a}) \quad (A-12)$$

Hence, the symbol J which we use when discussing the fully plastic case can consistently be identified with a far field value like  $J_f$ , although not

with the deformation theory value  $J_d$ . Further, (A-2) yields in the rigid-plastic case

$$\dot{\delta} = 0.37 b \dot{\theta} = 0.51 \dot{J}_f / \sigma_o \quad (A-13)$$

This is the origin of the value  $\alpha_{fy} \approx 0.51$  used in the text for the fully yielded bend specimen.

Also, we observe that since

$$\dot{J}_f = \dot{J}_d + J_d \dot{a}/b, \quad \text{or} \quad dJ_f/da = dJ_d/da + J_d/b \quad (A-14)$$

for the rigid-plastic bend specimen, we expect the same to be approximately valid for a fully yielded elastic-plastic bend specimen. Hence, if

$$T_f = \frac{E}{\sigma_o^2} \frac{dJ_f}{da} \quad \text{and} \quad T_d = \frac{E}{\sigma_o^2} \frac{dJ_d}{da}, \quad (A-15)$$

where  $T_f$  should be considered as the  $T$  of eqs. (36,37), then

$$T_d \approx T_f - EJ_d/\sigma_o^2 b \quad (A-16)$$

in this case. That is, the value of the tearing modulus is sensitive to the definition used for  $J$ , and  $T_d$  may turn negative with increasing growth while  $T_f$  remains positive. In particular, eq. (37) for the value of  $T$  (interpreted as  $T_f$ ) at the onset of growth in a fully plastic bend specimen with  $b = 25 J_{IC}/\sigma_o$  becomes, in terms of  $T_d$ ,

$$\begin{aligned}
 T_d &\approx [T_o + 7.8 \ln(E/31\sigma_o)] \alpha_{ssy}/\alpha_{fy} - E/25\sigma_o \\
 &\approx 1.3 T_o + 8 \quad , \quad \text{for } \sigma_o/E = 0.002 \quad \quad \quad (A-17) \\
 &\approx 1.3 T_o + 10 \quad , \quad \text{for } \sigma_o/E = 0.006
 \end{aligned}$$

where  $\alpha_{ssy}/\alpha_{fy}$  has been set equal to  $0.65/0.51 \approx 1.3$  again. Hence, even though  $J_d$  is fundamentally an incorrect parameter within our incremental, ideally plastic model, its use does seem under typical conditions to bring the fully plastic  $T$  value somewhat closer to  $T_o$ . In fact, if the differences between  $\alpha_{fy}$  and  $\alpha_{ssy}$  were neglected, the difference between  $T_d$  and  $T_o$  in the above expressions would be 2 and 6, respectively.

Finally, we remark that  $J_f$  does not seem to be the appropriate definition of  $J$  for all rigid-plastic specimens. For example, suppose the specimen in fig. 6 is considered to represent one-half of a double edge cracked tensile specimen, with cracks deep enough to validate the Prandtl field over the uncracked ligament, and let  $U$  be the extension of one end of the specimen relative to the other. Then it is straightforward to show [10] that the deformation theory value is

$$J_d = [(2+\pi)/\sqrt{3}] \sigma_o U = 2.97 \sigma_o U \quad , \quad \quad \quad (A-18)$$

whereas  $J_f$  does not seem to have any unique value for the case of a growing crack (due to non-uniqueness of the stress field in rigid regions of the specimen) for the contour  $\Gamma$  shown. In this case it is  $J_d$  which exhibits the desired feature that  $\dot{J}$  is independent of  $\dot{a}$ . Also, the rate of opening at the crack tip is [10]

$$\dot{\delta} = 2\dot{U} = 0.67 \dot{J}_d/\sigma_o \quad . \quad \quad \quad (A-19)$$

Hence  $\alpha_{fy} \approx 0.67$  in this case, which is very close to what we have estimated as the small scale yielding value. Thus, lessened differences between  $T$  and  $T_0$  are expected for this type of specimen, particularly when  $T$  is based on  $J_d$ .

Finally, for the center-cracked, rigid-plastic plane strain tensile specimen it is elementary to show that

$$J_d = J_f = (2\sigma_0/\sqrt{3})U, \quad (A-20)$$

provided that  $J_f$  is evaluated on a contour similar to that in fig. 6, and that the opening rate at the tip is

$$\dot{\delta} = \dot{U} = 0.87 \dot{J}/\sigma_0. \quad (A-21)$$

However, this specimen does not have a Prandtl-like stress state at its tip, and cannot be discussed in terms of the analysis in the body of the paper.

### Acknowledgement

This study was supported by the Department of Energy under contract EY-76-S-02-3084 with Brown University. In addition, T-L. Sham was supported in part by an EPRI subcontract from the General Electric Company to Brown, and the numerical results which we cite were obtained by computation at General Electric (Schenectady) under auspices of this subcontract. We are grateful to Drs. C-F. Shih of General Electric, A. Needleman of Brown, and E. P. Sorensen of Hibbitt-Karlsson, Inc. (Providence) for helpful discussions.

Additional note: Since presentation of the paper we learned of the work of L.I. Slepyan ("Growing crack during plane deformation of an elastic-plastic body", Izv. AN SSR. Mekhanika Tverdogo Tela, Vol. 9, pp. 57-67, 1974). Using methods of asymptotic analysis similar to those of [12] and, for the growing crack, [8] and [10], Slepyan determines the form of the near tip stress and deformation fields for a crack growing under steady state conditions in an ideally plastic Tresca material. He comes to the same conclusions as in [2] on the necessity of an elastic unloading zone of the form shown in fig. 1d. The results of [2] have a slight dependence of the unloading zone boundary angles  $\theta_1$ ,  $\theta_2$  on the Poisson ratio, since [2] is based on the Mises model, whereas Slepyan's work, based on the Tresca model, does not. But for  $\nu = 1/2$  the results are identical.

## References

1. Rice, J. R. and E. P. Sorensen, "Continuing crack tip deformation and fracture for plane strain crack growth in elastic-plastic solids," J. Mech. Phys. Solids 26, 1978, 163-186.
2. Drugan, W. J., and J. R. Rice, Research in preparation for publication, Brown University, Spring 1979.
3. Sorensen, E. P., "A numerical investigation of plane strain stable crack growth under small scale yielding conditions," in Proc. ASTM Symp. Elastic-Plastic Fracture (Atlanta, 1977), ASTM-STP, Philadelphia, in press.
4. Sham, T-L., "A finite element analysis of quasi-static crack growth in an elastic-perfectly plastic solid," Sc.M. Thesis, Brown University, Division of Engineering, March 1979.
5. Paris, P. C., Tada, H., Zahoor, A. and H. Ernst, "A treatment of the subject of tearing instability," U.S. Nuclear Regulatory Commission Report NUREG-0311, August, 1977 (available through National Technical Information Service, Springfield, VA).
6. Hutchinson, J. W. and P. C. Paris, "Stability analysis of J-controlled crack growth," Proc. ASTM Symposium on Elastic-Plastic Fracture (Atlanta, November, 1977), ASTM-STP in press. Amer. Soc. for Test. and Mat., Philadelphia.
7. Rice, J. R., "The mechanics of crack tip deformation and extension by fatigue," in Fatigue Crack Propagation, ASTM STP-415, 1967, pp. 247-311.
8. Rice, J. R., "Mathematical analysis in the mechanics of fracture," in Fracture: An Advanced Treatise, H. Liebowitz (ed.), vol. 2, Academic Press, 1968, 191-311.
9. Hutchinson, J. W., "Plastic stress and strain fields at a crack tip," J. Mech. Phys. Solids 16, 1968, 337-347.
10. Rice, J. R., "Elastic-plastic models for stable crack growth," in Mechanics and Mechanisms of Crack Growth (Proc. Conf. at Cambridge, England, April, 1973), M.J. May (ed.), British Steel Corporation Physical Metallurgy Centre Publication, 1974, 14-39.
11. Cherepanov, G. P., Mechanics of Brittle Fracture (in Russian), Gos. Izdat., Moscow, 1974, 271.
12. Rice, J. R. and D. M. Tracey, "Computational fracture mechanics," in Numerical and Computer Methods in Structural Mechanics, S.J. Fenves et al. (ed.), Academic Press, 1973, 585-623.
13. Hutchinson, J. W., "Singular behavior at the end of a tensile crack," J. Mech. Phys. Solids 16, 1968, 13-31.

14. Rice, J. R. and G. R. Rosengren, "*Plane strain deformation near a crack tip in a power law hardening material*," *J. Mech. Phys. Solids* 16, 1968, 1-12.
15. McClintock, F. A., "*Plasticity aspects of fracture*," in Fracture: An Advanced Treatise, H. Leibowitz (ed.), vol. 3, Academic Press, 1971, 47-225.
16. Shih, C. F., deLorenzi, H. G. and W. R. Andrews, "*Studies on crack initiation and stable crack growth*," in Proc. ASTM Symposium on Elastic-Plastic Fracture (Atlanta, 1977), ASTM-STP, Philadelphia, in press.



### Figure Captions

Fig. 1 Stress field at crack tip consists, in yielded sectors, of either (a) centered fan or (b) constant stress regions. The full Prandtl field (c) results for a stationary crack, at least at small scale yielding, but must be modified (d) with an elastic unloading sector for a growing crack.

Fig. 2 Comparison of crack tip stress state for a growing crack (dashed lines, based on field of fig. 1d) with the Prandtl field for a stationary crack (solid lines, based on field of fig. 1c). Stresses are made dimensionless by tensile yield strength.

Fig. 3 Opening profiles near the tips of growing cracks with various values of  $T \equiv (E/\sigma_o^2)dJ/da$ , and near a stationary crack tip; based on  $\alpha = 0.65$ ,  $\beta = 5$ ,  $R = 0.2EJ/\sigma_o^2$  ( $\approx$  plastic zone size).

Fig. 4 Finite element results for increments  $\Delta\delta$  of crack surface opening due to load increase at fixed crack length, based on finite element solution for small scale yielding with load history as shown. (a) Load increases following one-element steps of crack growth. (b) Last few increments of monotonic loading of stationary crack.

Fig. 5 Correlation of finite element results for crack opening  $\delta$ , in growth at constant  $J$ , with theoretical result. Each set of points corresponds to total  $\delta$  values, along the path of constant  $J$  growth, after a one-element growth step. Resulting estimates of  $\beta$  and  $R$  are shown.

Fig. 6 Speculation on the variation of  $R$  with  $J$  over the entire range of yielding. The linear variation at low  $J$  is expected to become non-linear as shown and to finally saturate in value (the level  $\approx 1/4$  is a guess) at general yielding.

Fig. 7 Crack growth criterion of RS requires that a critical opening  $\delta_c$  be maintained at small distance  $r_m$  behind the tip. As discussed at end of paper, the criterion is similar qualitatively to others based on other deformation parameters (e.g., plastic strain) of the near tip field.

Fig. 8 Predicted variation of  $J$  with  $a-a_0$  for small scale yielding. Curves are drawn for different values of  $T_0$ , which is the value of  $(E/\sigma_0^2)dJ/da$  at the onset of growth under small scale yielding conditions. Based on  $\alpha = 0.65$ ,  $\beta = 5.08$ . Growth criterion of RS can be stated in terms of the "macroscopic" parameters  $J_{IC}$  and  $T_0$ , rather than the "microscopic" parameters of Fig. 7. Note that  $a-a_0$  is scaled by what is, approximately, the maximum plastic zone radius at the onset of growth.

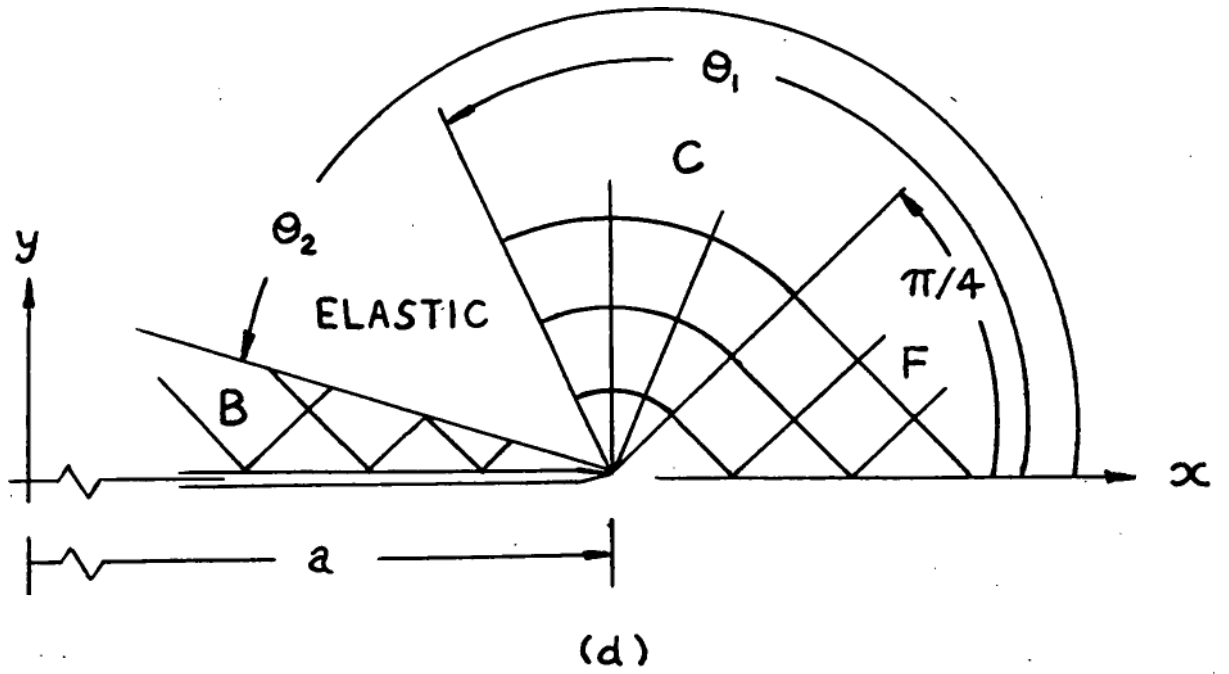
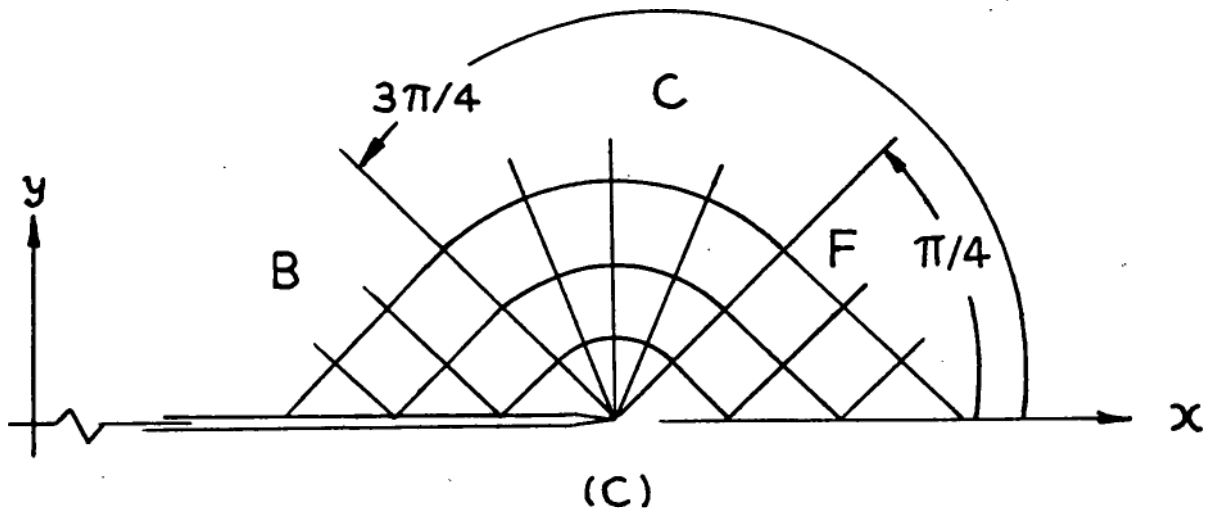
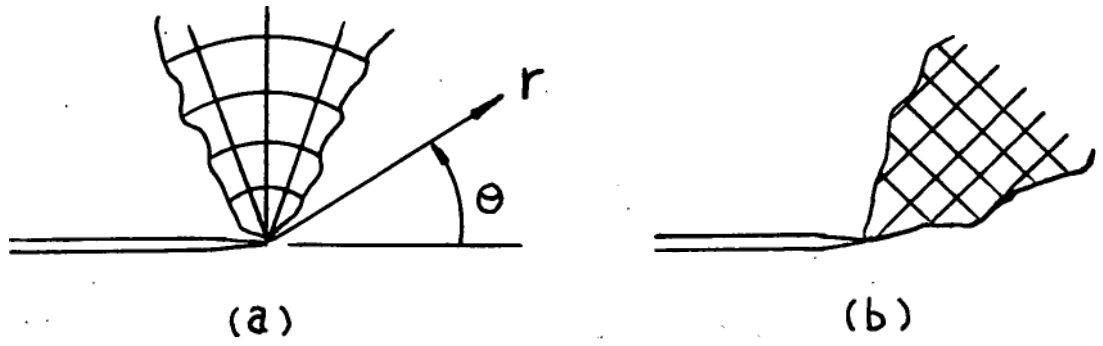
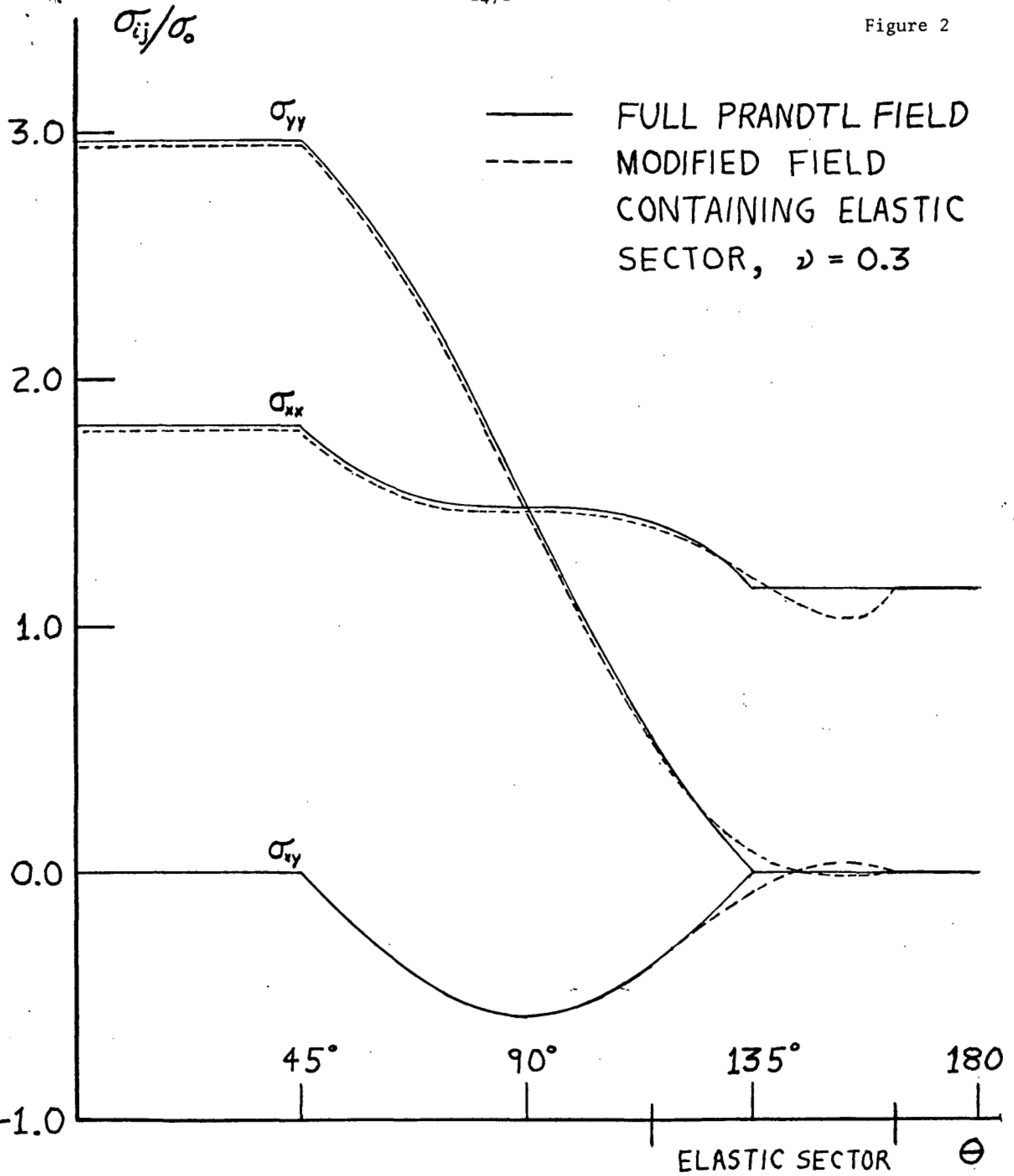
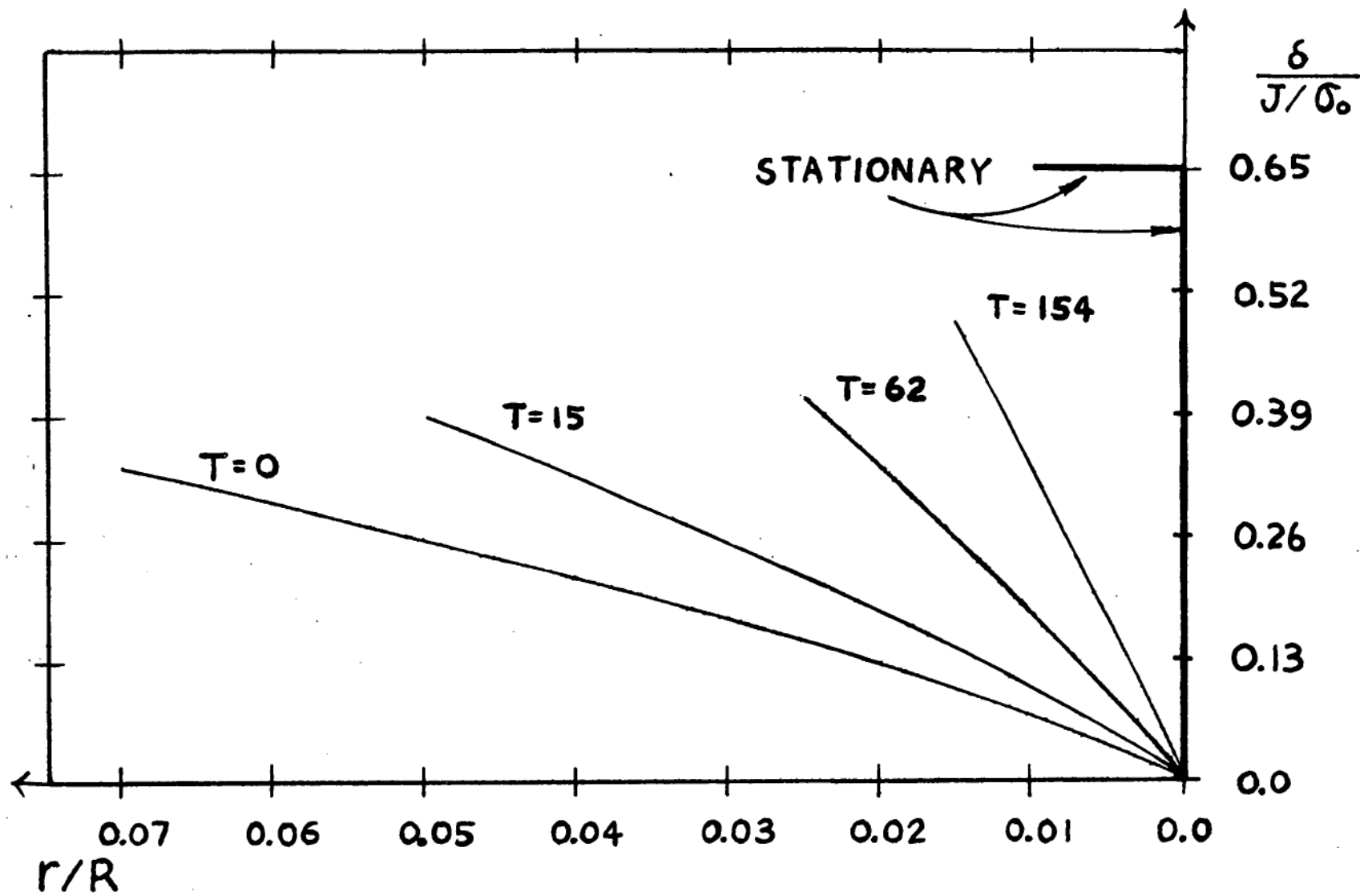


Figure 2





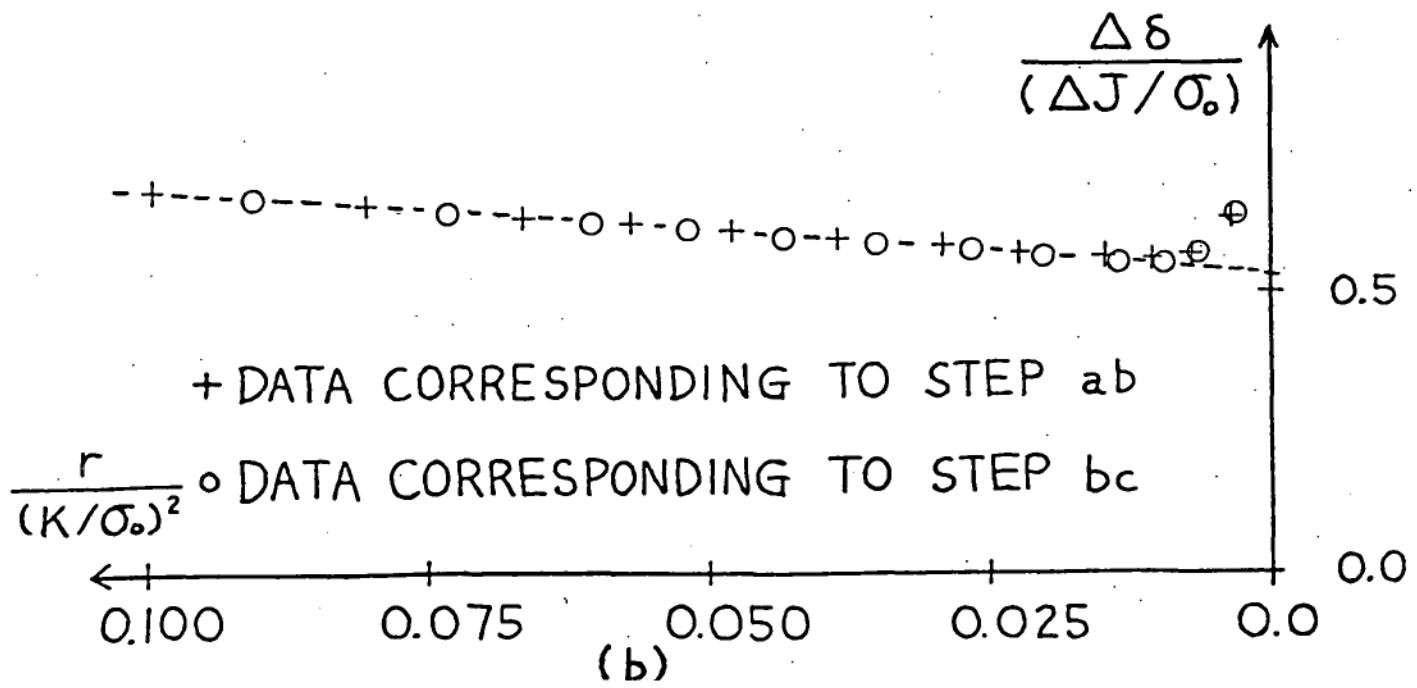
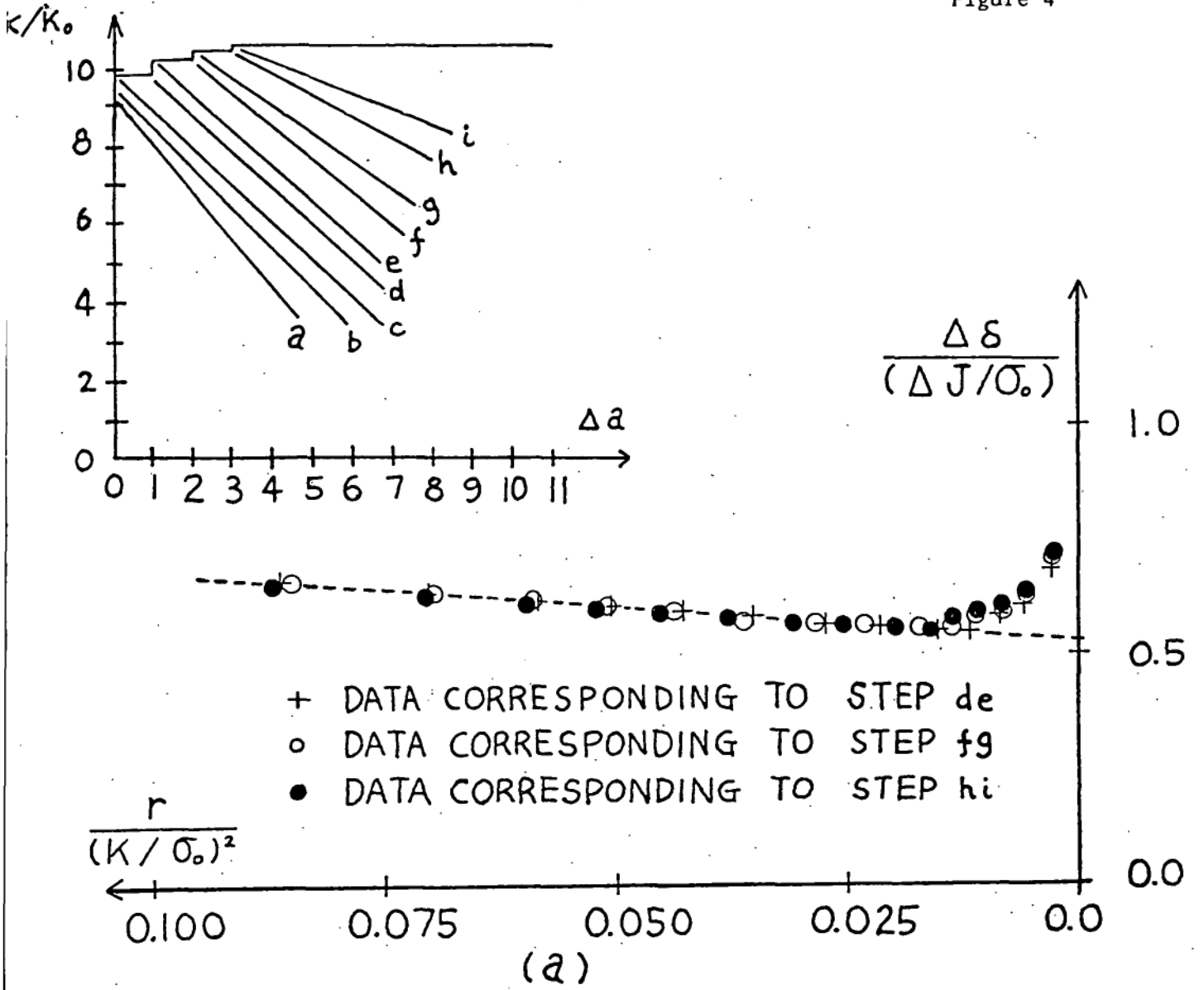


Figure 9

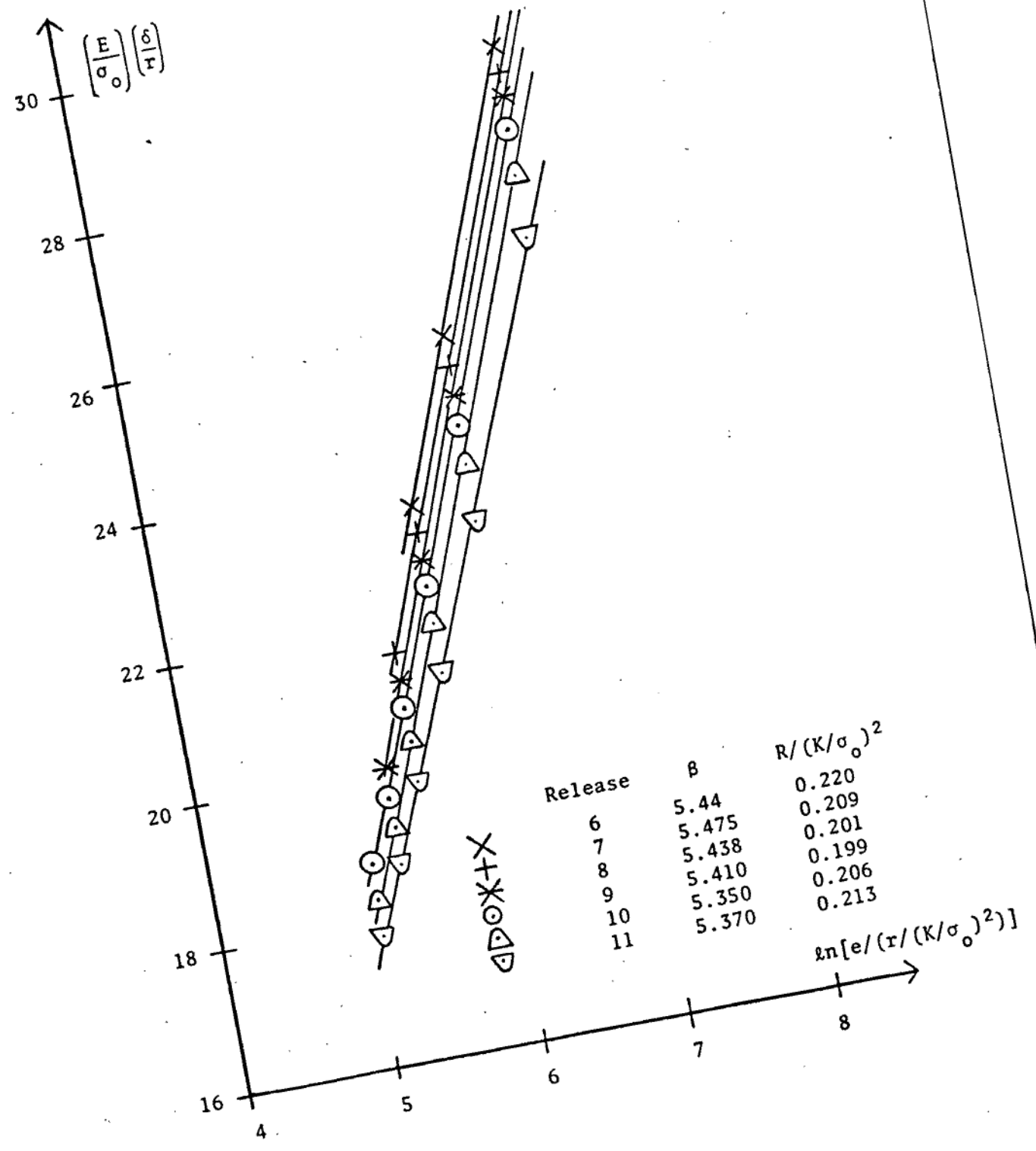


Figure 6

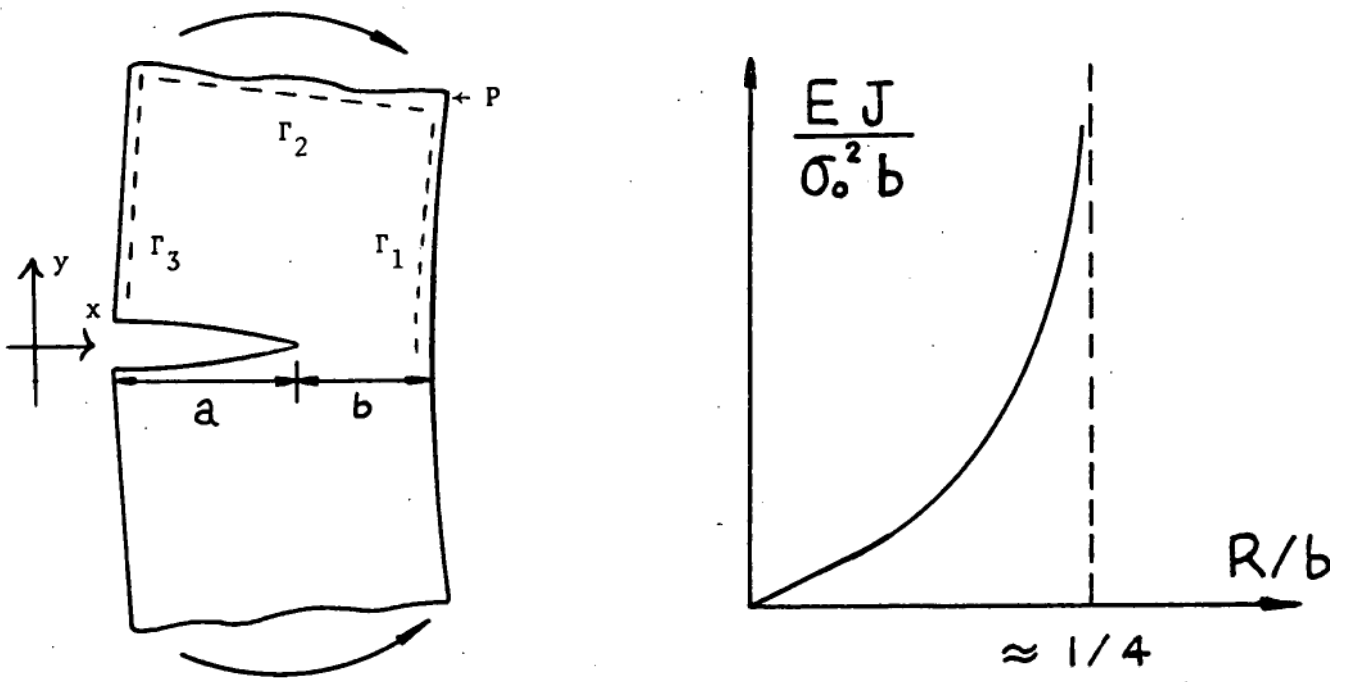


Figure 7

